arXiv:astro-ph/9602082v1 16 Feb 1996

Abundance and Clustering of C IV Absorption Systems in the SCDM, LCDM and CHDM Models

Hongguang Bi* and Li-Zhi Fang

Department of Physics, University of Arizona

Tucson, AZ 85721

All correspondence to: L.Z. Fang

Abstract

We have developed a method for calculating the two-point correlation function of nonlinearly evolved mass and collapsed halos in the Press-Schechter formalism. The nonlinear gravitational interaction is treated as the sum of various individual spherical top-hat clustering. Because no collapsed halo of mass M can exist in initial regions (or top-hat spheres) of mass less than M, the bias that massive halos have stronger correlation than the background mass can be naturally introduced.

We apply this method to derive constraints on popular dark-matter models from the spatial number density and the correlation function of C IV absorption systems in QSO spectra. Considering C IV systems should be hosted by collapsed halos, one can obtain an upper limit to the threshold mass of the collapsed halos by requiring their number density to be larger than that of observed C IV systems. On the other hand, in order to explain the observed clustering of C IV systems, a lower limit to the threshold mass will be set for the hosting halos. We found that the standard cold dark matter (SCDM) model and the low-density flat universe with a cosmological constant Λ_0 (LCDM) are consistent with the abundance and clustering of C IV systems. However, the two cold-plus-hot dark matter models (CHDMs) with the cosmological parameters $(\Omega_c + \Omega_b)/\Omega_h = 0.7/0.3$ and 0.8/0.2, respectively, have difficulty passing the two tests simultaneously. In these models, in order to have enough collapsed halos to host C IV systems, the threshold mass of the halos can not be greater than $10^{11}\ M_\odot$. But in order to agree with the two-point correlation function on the scales of $\Delta v \sim 300 - 1,000$ km/s, the threshold mass should be larger than $10^{12}\ M_\odot$.

Subject headings: cosmology: theory — dark matter — quasars: absorption lines

1. Introduction

It has been recognized that the abundance, i.e. the spatial number density, of moderate and high redshift objects can put promising constraints on models of structure formation in the universe. For instance, an N-body simulation has shown that the "standard" cold-plus-hot dark matter model (CHDM) of $\Omega_c/\Omega_h/\Omega_b = 0.6/0.3/0.1$, here c, b and h denoting cold, baryonic and hot respectively, lacks the perturbations necessary to form clusters before $z \geq 0.5$, although it can produce a proper number of clusters at $z = 0$ (Jing & Fang 1994). In contrast, the low density, flat cold-dark-matter model (LCDM) can produce enough clusters at both $z \geq 0.5$ and $z = 0$. Hence, the abundance of $z \geq 0.5$ clusters is a useful quantity for discriminating between the CHDM model and the LCDM model. Another example is the damped Lyα systems which are rich in QSO absorption spectra at $z \geq 2$. Both the Press-Schechter formalism and N-body simulations indicated that the "standard" CHDM model has difficulty explaining these systems (Mo & Miralda-Escudé 1994; Ma & Bertschinger 1994; Klypin et al. 1995). A simulation of the Lyα forest has shown that the predicted number of forest lines is less than what is observed by at least one order of magnitude even if extreme parameters are used in this model (Bi, Ge & Fang 1995).

Among the various samples of high-redshift objects, those selected from absorption systems in QSO spectra are relatively uniform and numerous and can be used to provide stringent constraints on different theoretical models. However, a common problem of 1-D samples is the lack of information on the size and geometry the objects. Calculating 3-D abundances from 1-D data requires assumptions about the objects' shape. Obviously, this leads to an uncertainty in the results. This difficulty is partly overcome in this study. We propose to test models not only by abundance, but also by clustering property of a high-redshift sample. Like abundance, clustering of collapsed halos depends also on their

mass and/or size, so adding a clustering test will reduce the unknown parameters. In some cases, conclusions could even be completely free from these parameters.

The present analytical study is based on the Press-Schechter formalism (Press & Schechter 1974, hereafter PS) that has been found to be successful in describing the mean number density of collapsed virial halos with different mass threshold at high redshifts. The spatial range in our study covers from redshift 2 to 4, and the correlation scales are from 300 to tens thousand km s^{-1}, which are otherwise difficult to handle by current gas simulations.

For our goal, we need a method to calculate the correlation function of collapsed halos in the PS formalism. The existing PS theory does not yet tell us about the correlation function. In the first part of this paper, we will discuss how to extend the PS formalism to obtain the spatial correlation function of nonlinearly evolved mass and collapsed halos. A similar problem has been studied recently by Mo & White (1995). The idea is that the gravitational clustering from given initial density fluctuations can be approximately treated as many individual top-hat-evolved spherical regions. The mass correlation can then be deduced from the mass distribution within such regions. The bias of halo autocorrelations with respect to their masses is derived by assuming that no halo of mass M can exist in uncollapsed regions of mass less than M. This approximation is found to be in good agreement with the linear approximation on large scales, and to be consistent with the empirical formalism on scales where the non-linear effects are significant (e.g. Hamilton et al. 1991).

In the second part, we apply the developed method to C IV absorption systems in QSO spectra. We compare the abundance and clustering of collapsed halos in theoretical models with those given by real C IV observations. Among high-redshift absorption samples, only metal absorption systems and Lyα forest lines can provide the statistics of both linear number densities and spatial correlation functions (Sargent, Boksenberg & Steidel 1988). Lyα absorption lines are most likely from clouds with large size and low column density

which are neither virialized nor completely confined (Bechtold et al. 1994; Dinshaw et al. 1994). Hence, we should not simply identify their hosts as collapsed halos. In contrast, metal systems are generally believed to be from huge halos surrounding galaxies (Wolfe 1993). Because stars were certainly formed in the systems, they must have undergone non-linear collapse. Therefore, metal absorption lines are probably the only available 1-D sample for our purpose.

Observationally, metal absorption systems contain Mg II selected systems, C IV selected systems, and Lyman limit systems. However, the categories of absorbers identified by different systems are not orthogonal with each other (Wolfe 1993). The Lyman limit systems are almost indistinguishable from the Mg II systems, and most Mg II systems exhibit C IV, too. Most metal systems were obtained from ground observations. The C IV systems are usually found in the redshift interval $1.2 \leq z \leq 4.1$, and the MgII systems in $0.2 \leq z \leq 1.9$. Because we are interested mainly in the physics at high redshift ($z > 2$), only C IV absorption systems will be investigated.

It should be pointed out that, like other studies of high-redshift objects based on the PS formalism, our goal is not to model the details of the C IV systems, instead it is to use the number of C IV systems as a *lower limit* to the number of corresponding collapsed halos. It is believed that the presence of C IV depends on the chemical abundance of heavy elements and on the ionization state of baryonic gas (Bergeron et al. 1994). Observations have shown an evolution in these chemical properties (Steidel 1990). It indicates that C IV systems should be located in areas in which chemical abundance evolution has already taken place. Therefore, C IV systems should be harbored in collapsed PS halos. Thus, a reasonable constraint on models of structure formation is that the predicted number of collapsed PS halos should be greater than that of observed C IV systems.

In §2, we describe the PS method for calculating the spatial number density of collapsed halos, then we extend this idea to general uncollapsed regions and derive an approximate expression for the correlation functions of mass and halos. In §3, the four SCDM, LCDM

and CHDM models of structure formation are tested based on their predictions of the abundance and clustering of collapsed halos. We discuss how observations can be compared with the predictions. Finally, §4 gives discussion and conclusions.

2. Method

2.1 Number density of collapsed halos

The spatial number density of collapsed halos can be calculated from the standard PS theory. We define $\delta(\mathbf{x}, z)$ to be the 3-D density fluctuation field of dark matter extrapolated to redshift z assuming linear evolution. A density field $\delta_R(\mathbf{x})$, representing the smoothed fluctuation on scale R, can be derived from $\delta(\mathbf{x})$ by

$$\delta_R(\mathbf{x}) = \frac{1}{V_R} \int \delta(\mathbf{x}_1) W(R; \mathbf{x}_1 - \mathbf{x}) d\mathbf{x}_1, \tag{1}$$

where the function $W(R; \mathbf{x}_1 - \mathbf{x})$ is the top-hat window for the comoving volume $V_R = 4\pi R^3/3$. In the $\Omega = 1$ Einstein-de Sitter universe, the variance of δ_R evolves as $\sigma_R^2 \propto (1+z)^{-2}$. The total mass within V_R is $M = V_R \rho_0$, where ρ_0 is the present cosmological density when the scaling factor of the universe is set to be unity at $z = 0$.

For a Gaussian field, the fraction of the total mass $\rho_0 \Delta\mathbf{x}$ having fluctuations larger than a given δ_c in an arbitrary spatial domain $\Delta\mathbf{x}$ is

$$F_R = \int_{\delta_c}^{\infty} \frac{1}{\sqrt{2\pi}\sigma_R} \exp\left(-\frac{\delta_R^2}{2\sigma_R^2}\right) d\delta_R. \tag{2}$$

Therefore, if we take $\delta_c = 1.686$, the critical value for collapse in the top-hat evolution, $F_R \cdot \rho_0 \Delta\mathbf{x}$ should be identified as the sum of masses of all collapsed halos, each of which is greater than $M = V_R \rho_0$. The differential $-\frac{\partial}{\partial M}(F_R \rho_0 \Delta\mathbf{x}) dM$ gives the total mass of collapsed halos in the range M to $M + dM$. Hence, if we define $n_c(M)dM$ to be the spatial number density of halos between M and $M + dM$, we have

$$-\frac{\partial}{\partial M}(F_R \rho_0 \Delta\mathbf{x}) dM = n_c(M) dM \cdot M \Delta\mathbf{x}, \tag{3}$$

where we use the subscript c in n_c to emphasize that it is for collapsed halos.

Because the cloud-in-cloud problem has not been appropriately considered in Eq. (3), the original PS theory takes an ad hoc assumption that the above defined n_c should be multiplied by a factor of 2 (see discussions in Bond et al. 1991). The normalization $\int_0^\infty n_c(M)MdM = \rho_0$ can thus be fulfilled when $\sigma_R(R \to 0) = \infty$. One has finally

$$n_c(M) = -\frac{\rho_0}{M}\frac{\partial}{\partial M}\mathrm{erfc}\left(\frac{\delta_R}{\sqrt{2}\sigma_R}\right), \tag{4}$$

where erfc(x) is the complementary error function. The cumulative number density, $N_c(M)$, of all halos greater than M should be

$$N_c(M) = \int_M^\infty n_c(M_1)dM_1. \tag{5}$$

The abundance of halos calculated from Eq. (5) has been verified by a number of N-body simulations (e.g. Efstathiou et al. 1988; Lacey & Cole 1994; Jing & Fang 1994).

2.2 δ_c in the flat universe with a cosmological constant

The critical value of collapse, $\delta_c = 1.686$, is derived in the Einstein-de Sitter model. Now, we calculate δ_c in the flat $\Lambda \neq 0$ universe. In this case, the evolution of a spherical volume with mass M should be described by a Newtonian equation in the proper coordinate (Peebles 1984) :

$$\frac{d^2r}{dt^2} = -\frac{GM}{r^2} + \frac{1}{3}\Lambda r, \tag{6}$$

where $\Lambda = (1-\Omega)3H_0^2$. Eq.(6) can be integrated to give

$$\left(\frac{dr}{dt}\right)^2 = 2GM(\frac{1}{r} - \frac{1}{r_m}) + (1-\Omega)H_0^2(r^2 - r_m^2), \tag{7}$$

where r_m denotes the radius when the sphere reaches its maximum size. From Eq. (7), one has

$$t = \int_0^r [2GM(\frac{1}{r} - \frac{1}{r_m}) + (1-\Omega)H_0^2(r^2 - r_m^2)]^{-1/2}dr,$$

$$= \frac{1}{\sqrt{1-\Omega}H_0}\int_0^{r/r_m} y^{\frac{1}{2}}(1-y)^{-\frac{1}{2}}(c_0-y^2-y)^{-1/2}dy, \tag{8}$$

where $c_0 \equiv 2GM/(1-\Omega)H_0^2 r_m^3$.

If we define t_m to be the cosmic time at which the sphere is at its maximum radius r_m, the collapse time t_c of this sphere is twice t_m. Therefore, taking $t_m = t_c/2$ in Eq. (8), we find

$$t_c(c_0) = \frac{2}{\sqrt{1-\Omega}H_0}\int_0^1 y^{\frac{1}{2}}(1-y)^{-\frac{1}{2}}(c_0-y^2-y)^{-1/2}dy. \tag{9}$$

The redshift z_c that is a function of c_0 can be found according to the $z-t$ relationship in the flat universe:

$$H_0 t = \frac{2}{3(1-\Omega)^{1/2}}\sinh^{-1}[\sqrt{\frac{1-\Omega}{\Omega}}(1+z)^{-3/2}]. \tag{10}$$

At the time of recombination t_d, the radius of the sphere r_d is much less than r_m, so the integration in Eq. (8) can be approximated as

$$t_d = \frac{1}{\sqrt{1-\Omega}H_0}\left[\frac{2}{3}(\frac{r_d}{r_m})^{3/2} + \frac{1+c_0}{2c_0}\frac{2}{5}(\frac{r_d}{r_m})^{5/2}\right]. \tag{11}$$

Again using the $z-t$ relationship, one can write the density perturbation in the sphere at t_d, $\delta_d = M/\frac{4\pi}{3}r_d^3(1+z_d)^3\rho_0 - 1$, as

$$\delta_d(c_0) = \frac{3c_0(1-\Omega)H_0^2 r_m^3}{8G\pi r_d^3(1+z_d)^3\rho_0} - 1 \simeq \frac{1+c_0}{c_0}\frac{3}{5}\left[\frac{(1-\Omega)c_0}{\Omega}\right]^{1/3}\frac{1}{1+z_d}. \tag{12}$$

Since z_c depends only on c_0, we can write the above c_0 as a function of z_d, i.e. $c_0 = c_0(z_d)$.

Using this initial density fluctuation, one obtains the subsequent linear evolution at the epoch of collapse t_c :

$$\delta_c(z_c) = D(z_c)(1+z_d)\delta_d = \tag{13}$$

$$[\Omega(1+z_c)^3 + 1 - \Omega]^{1/2}\frac{3}{5}\frac{1+c_0(z_c)}{c_0(z_c)}\left[\frac{(1-\Omega)c_0(z_c)}{\Omega}\right]^{1/3}\int_{z_c}^{\infty}\frac{(1+z)dz}{[\Omega(1+z)^3+1-\Omega]^{3/2}}$$

where $D(z)$ is the linear growing factor in the LCDM model.

Fig. 1 shows $\delta_c(z_c)$ vs. z_c for $\Omega = 0.9,\ 0.7,\ 0.5,\ 0.3,\ 0.1$. All of the $\delta_c(z_c)$ curves are approaching the traditional value 1.686; there is no noticeable difference among the thresholds at redshifts $z \geq 1$. This indicates that the trajectory of the top-hat collapse in the flat Λ universe is very well described by simply the Einstein-de Sitter universe at high redshift, so we will take $\delta_c = 1.686$ in the following calculations.

2.3 Number density of uncollapsed regions

As pointed out by Mo & White (1995), the nonlinear effect of gravitational clustering of dark matter can be treated as the sum of various individual top-hat spheres including both collapsed halos and uncollapsed regions. An uncollapsed region (sometimes called *PS spherical region* or *uncollapsed sphere*; *halo* is usually a terminology for collapsed objects) corresponds to linear fluctuations not yet reaching the threshold 1.686 at the redshift considered. Therefore, we can apply the same statistical method as that used by Press and Schechter for collapsed halos to uncollapsed regions. Following §2.1, we first calculate the number density of uncollapsed regions.

The evolution of a spherical region of radius $r = r_d$ at recombination $z = z_d$ is described by Eq. (6). In the Einstein-de Sitter case, the solution of Eq. (6) can be expressed analytically as

$$r = \frac{3}{10}\frac{r_0}{\delta_0}(1-\cos\theta), \qquad \frac{1}{1+z} = \frac{3\times 6^{2/3}}{20\delta_0}(\theta-\sin\theta)^{2/3} \tag{14}$$

for $\delta_0 > 0$, and

$$r = \frac{3}{10}\frac{r_0}{\delta_0}(1-\cosh\theta), \qquad \frac{1}{1+z} = -\frac{3\times 6^{2/3}}{20\delta_0}(\sinh\theta-\theta)^{2/3} \tag{15}$$

for $\delta_0 < 0$, where $r_0 \equiv (1+z_d)r_d$ and $\delta_0 \equiv (1+z_d)\delta_d$ are, respectively, the linear extrapolation of the radius and density contrast to $z = 0$. Note that the mass of this sphere is then given by $M = \frac{4\pi}{3}(1+z_d)^3 r_d^3 \rho_0(1+\delta_d)$.

Let's consider an arbitrary spherical volume of radius r at redshift z. Matter in this volume can come from various initial spheres of different r_0 and δ_0. For a given r and

z, one can find the relationship between r_0 and δ_0 from Eqs. (14) and (15). This is $\frac{\delta_0}{\delta_c(1+z)} = f(\frac{r(1+z)}{r_0})$. Function $f(x)$ is plotted in Fig. 2. The meaning of the figure is straightforward. When $\delta_0 = 0$, one has $r = r_0/(1+z)$, i.e. the evolution of this region is just comoving. An initial sphere with perturbation $\delta_0 > 0$ will evolve into the radius $r < r_0/(1+z)$ at redshift z. For $\delta_0 < 0$, it will evolve into $r > r_0/(1+z)$. All initial spheres with $\delta_0 > \delta_c(1+z)$ result in $r = 0$, i.e. they are collapsed halos.

One can consider the initial density field as a system consisting of many spheres, each of which has the same radius r_0 but various density contrasts δ_0. Similar to Eq. (2), the mass fraction of the spheres greater than δ_0 is given by

$$\int_{\delta_0}^{\infty} \frac{1}{\sqrt{2\pi}\sigma_{r_0}} \exp\left(-\frac{\delta^2}{2\sigma_{r_0}^2}\right) d\delta \tag{16}$$

where $\sigma_{r_0}^2$ is the variance of density perturbation on scale r_0. Because a spherical region of δ_0 and r_0 will evolve into r at z, initial spherical regions of $\delta \geq \delta_0$ and r_0 will evolve into radii less than r at z. Therefore, the comoving number density of the uncollapsed PS spheres with mass in $M_0 \to M_0 + dM_0$ (or radii $r_0 \to r_0 + dr_0$) at recombination, which are spheres with radius less than r at z, is given by

$$n(M_0)dM_0 = -\frac{\rho_0}{M_0}\frac{1}{2}\frac{\partial}{\partial M_0}\mathrm{erfc}\left[\frac{\delta_0}{\sqrt{2}\sigma(r_0)}\right] dM_0, \tag{17}$$

where we use the subscript 0 in M_0 to emphasis that it is for the uncollapsed regions, not only the collapsed halos discussed in §2.1. It should be pointed out that Eq. (16) contains spheres of both $\delta_0 < \delta_c(1+z)$ and $\delta_0 > \delta_c(1+z)$. Therefore, $n(M_0)dM_0$, in fact, includes both uncollapsed regions and collapsed halos. Since initial spherical regions entirely cover the density field, $n(M_0)$ should satisfy the normalization condition $\rho = \int_0^\infty n(M_0)M_0 dM_0 = \rho_0$ for all r and z. It is easy to verify this normalization from Eqs. (16) and (17).

2.4 Mass-correlation function

Since $n(M_0)dM_0$ gives the number density of uncollapsed spherical regions with mass

$M_0 \to M_0 + dM_0$ and radii $\leq r$ at z, the fraction of regions with radius $r \to r + dr$ can be obtained by differentiating $n(M_0)$ with respect to $V = 4\pi r^3/3$. Defining $m(M_0, V)dM_0dV$ to be the number density of the regions with radius $r \to r + dr$ or $V \to V + dV$, where $dV = 4\pi r^2 dr$, we have

$$\begin{aligned} m(M_0, V) &= \frac{\partial}{\partial V} n(M_0) \\ &= -\frac{\rho_0}{M_0}\frac{1}{2}\frac{\partial^2}{\partial M_0 \partial V}\mathrm{erfc}\left[\frac{\delta_0}{\sqrt{2}\sigma(r_0)}\right]. \end{aligned} \tag{18}$$

Therefore, the total number of such spherical regions in an arbitrary volume dV_1 should on average be given by $m(M_0, V)dM_0dVdV_1$.

The mass correlation function $\xi(r)$ can be defined as the relative enhancement of mass density in the spherical shell $r \to r + dr$ around dV_1. Only the spheres with radius $r \to r + dr$ can contribute to this enhancement. The mean enhancement of each M_0 sphere is approximately described by its mass variance $M_0^2\sigma^2(M_0, z)$, where σ^2 is the variance of the linear density contrast extrapolated to z. Therefore, the mass correlation function can be expressed as

$$\begin{aligned} \xi(r, z) &= \frac{\int_0^\infty m(M_0, V)dM_0dVdV_1 \cdot M_0^2\sigma^2(M_0, z)}{\rho_0 dV \cdot \rho_0 dV_1} \\ &= \int_0^\infty dM_0 m(M_0, V)V_0^2\sigma^2(M_0, z). \end{aligned} \tag{19}$$

The factors $\rho_0 dV$ and $\rho_0 dV_1$ are the mean mass in the spherical shell $r \to r + dr$ and the volume dV_1, respectively. Obviously, in deriving Eq. (19), we assumed that there is no correlation among the initial spheres, so the mass fluctuation in the shell is simply given by the sum of the individual components.

We can check the approximation of Eq. (19) by comparing it with the linear approximation and other empirical non-linear formulae. First, because the mass correlation function is very well described by the linear approximation on large scales, Eq. (19) should be equal to the linear correlation function when r is large. The integrated mass

correlation function $\overline{\xi}$ that is defined by

$$\overline{\xi}(r) = \frac{1}{V}\int_0^V \xi(V_1)dV_1, \qquad \xi(r) = \frac{\partial}{\partial V}(V\overline{\xi}(r)) \tag{20}$$

is shown in Fig. 3 for the SCDM, LCDM, CHDM1 and CHDM2 models respectively at $z = 2.8$. The solid lines in Fig. 3 represent our integrated correlation function from Eq.(19). The dotted lines in Fig. 3 are the linear approximation that matches Eq. (19) exactly on large scales.

The dashed line at the upper left of Fig. 3, i.e. in the SCDM model, is the empirical correlation function of Hamilton et al. (1991) fitted to early N-body simulation results in the SCDM model. Our approximation has nonlinear clustering behavior similar to theirs except for higher correlations on small scales. Since there has been discussion as to whether early N-body simulations underestimated the correlation function on the smallest scales, a further judgment on these two approximations should be done by simulations with higher resolution.

2.5 Correlation functions of collapsed halos

We now consider the correlation function of collapsed halos. From Eq. (5), the number of collapsed halos in an arbitrary volume V_0 is $N_c(M)V_0$. However, this is not the number *within* uncollapsed spheres which we discussed in the last two sections, because it is impossible that a collapsed halo can form from uncollapsed regions if the mass of the initial sphere is less than the mass of the collapsed halo.

To avoid this difficulty, we require that inside an uncollapsed sphere of mass M_0, the number density of collapsed halos is zero if their mass M is greater than M_0, or is proportional to N_c if their mass M is less than M_0. The number density of collapsed halos inside an PS sphere is thus given by

$$\mathcal{N}_c(M, M_0) = \begin{cases} AN_c(M) & \text{for } M \le M_0, \\ 0 & \text{for } M > M_0, \end{cases} \tag{21}$$

where the constant $A \geq 1$ is introduced to maintain the normalization condition

$$\int_0^\infty \mathcal{N}_c V_0 n(M_0) dM_0 = N_c. \tag{22}$$

Therefore, we have $A = 2/\mathrm{erfc}[\delta_0(r_c)/\sigma(r_c)]$ and $r_c = (3M/4\pi\rho_0)^{1/3}$.

Obviously, Eq. (21) is a simplified description of geometric bias (Kaiser 1984). Since the whole density field can be covered by spherical regions, every halo should be contained in a proper sphere. Massive collapsed halos can form only in massive uncollapsed spheres. Therefore, the probability of finding a collapsed halo in a massive uncollapsed sphere should be higher than in an average arbitrary volume by the factor $A \geq 1$. This effect will enhance the spatial correlation of massive halos.

As in §2.4, we consider a typical spherical shell $dV = 4\pi r^2 dr$. The total number of uncollapsed regions with radii $r \to r + dr$ and masses $M_0 \to M_0 + dM_0$ in the volume dV_1 is $m(M_0, V) dM_0 dV dV_1$. The total number of collapsed halos greater than M in each V_0 sphere is $\mathcal{N}_c(M) V_0$, and the variance of the number is $(\mathcal{N}_c V_0)^2 \sigma^2(r_0)$. Therefore, the correlation function of collapsed halos with mass larger than M can be expressed as

$$\begin{aligned} \xi(r; > M) &= \frac{\int_M^\infty dM_0 m(M_0, V) dV dV_1 \cdot (\mathcal{N}_c V_0)^2 \sigma^2(M_0, z)}{dV N_c \cdot dV_1 N_c} \\ &= A^2 \int_M^\infty dM_0 m(M_0, V) V_0^2 \sigma^2(M_0, z) \end{aligned} \tag{23}$$

where we implicitly assume that in uncollapsed regions, the collapsed halos have the same linear variance as the mass.

3. Application to C IV systems

We will concentrate on four models of structure formation: SCDM, LCDM, CHDM1 and CHDM2. The parameters of these models are listed in Table 1, including the Hubble constant h in the unit of 100 km s^{-1} Mpc^{-1}, the cosmological density parameters Ω, the cosmological constant Λ_0, and the quadrupole anisotropy Q_{rms} of the cosmic microwave background radiation used for the normalization of the linear spectrum. The parameters

are quite standard for these models. The linear transfer functions of the SCDM and the LCDM models are taken from Bardeen et al. (1986) and that of the CHDMs from Klypin et al. (1993). For all four models, we have assumed the Harrison-Zel'dovich primordial power spectrum. It is worth pointing out that the Q_{rms} normalization is compatible with the clustering of nearby galaxies in the LCDM, CHDM1 and CHDM2 models, but is too high for the SCDM model.

Part of the motivation for the two CHDM models comes from the possible non-zero rest mass of neutrinos. It has been claimed that the sum of the neutrino masses might be in the range 3.5 eV $< \sum m_{\nu i} <$ 6 eV (e.g. Louis 1994). Therefore, the allowed range for the neutrino density would be $0.2 \leq \Omega_\nu \leq 0.3$ when $h = 0.5$. The density parameters of the CHDM1 and CHDM2 models are taken to be the maximum and minimum of this range.

3.1 Abundance of possible hosts of C IV systems

The redshift evolution of the number density, $N_c(\geq M)$, of collapsed halos with mass greater than a given M are shown in Figs. 4a-d. The eight curves in each figure correspond to $M = 10^{10+n0.5}\ M_\odot$, with $n = 0, 1...7$ from top to bottom.

As discussed in §1, QSO metal absorption systems should be hosted by collapsed halos, because only in such regions can the formation of stars and evolution of heavy elements be taking place. Therefore, the number of the observed C IV systems can be used as a lower limit to the number of collapsed holes.

The number density of C IV systems is plotted as crosses in Fig. 4. The 3-D densities in the middle of the diagram were deduced from the observed line-of-sight number density (Steidel 1990) under the assumption that each absorber is spherical and has a radius of 39 h^{-1} kpc (Crotts et al. 1994). To consider the effect of uncertainties in the radius, we also plot in Fig. 4 the 3-D number densities if the radius is 5 times less than, and 5 times greater than 39 h^{-1} kpc. These are the upper set of points (8.0 h^{-1} kpc) and the lower

set of points (195 h^{-1} kpc), respectively. The factor of 5 might be enough to account for uncertainties in the measurement of the radius. It would be safely to use the data corresponding to the 195 h^{-1}kpc radius as the lower limit to the real number.

From Fig. 4, one sees that the possible hosts of C IV systems in the SCDM and LCDM models should have a mass threshold of about $10^{12.5}$ $M_\odot$. Say, that the number density of $M > 10^{12.5}$ $M_\odot$ collapsed halos is great enough to fit with the observed C IV lines. Because the lower the mass threshold, the more the collapsed halos, any mass threshold less than $10^{12.5}$ $M_\odot$ is allowed by the observation. In the CHDM1 and CHDM2 models, the number densities of collapsed halos are much less than those in the SCDM and LCDM models. In order to have enough collapsed halos hosting C IV systems, one has to choose much smaller mass thresholds. Figs. 4c and 4d showed that the assumed C IV halos should have a mass threshold as low as 10^{11} $M_\odot$ if the 195 h^{-1} kpc radius is used, or as low as $10^{9.5}$ $M_\odot$ for the 39 h^{-1} kpc radius. This mass threshold is about one and a half orders of magnitude lower than that in the SCDM and LCDM models. We conclude that in the CHDM models, the halos that host C IV must have masses as, at least, low as 10^{11} $M_\odot$.

3.2 Correlation functions of collapsed halos at high redshifts

Using the approximation of Eq. (23), we present the correlation function $\xi(r, \geq M)$ for collapsed halos in the SCDM, LCDM, CHDM1 and CHDM2 models in Fig. 5a-d. The mass threshold M is taken to be $10^{10+n0.5}$ $M_\odot$. The eight curves in each model correspond to $n = 0, ...7$ from left to right, respectively.

The histogram with error bars in Fig. 5 is the measured line-of-sight correlation function of C IV absorption systems on scales from $\Delta v \sim 300$ to 1,000 km s^{-1} (Sargent et al. 1988). C IV pairs with velocity differences less than 300 km s^{-1} probably do not represent large-scale clustering, but the internal structures of the host galaxies. The peculiar velocities of the C IV absorbers may also significantly contaminate the spatial correlations

on scales less than the velocity dispersion. Therefore, the correlations below 300 km s^{-1} have not been shown in Fig. 5. Since the radii of the halos (39 h^{-1} kpc or even 195 h^{-1} kpc), are much smaller than the scales being studied ($\geq$ 300 km s^{-1}), the 3-D correlation function is almost the same as that in 1-D. Therefore, one can directly compare the observed 1-D correlation length with theory.

Fig. 5a shows that the correlation function of $M \geq 10^{12} M_{\odot}$ halos in the SCDM model provide a good fit to the observational data. The halos are also well within the upper limit of the mass threshold, $10^{12} M_{\odot}$, derived in the last section. The same can be said for the LCDM model. In fact, SCDM and LCDM are indistinguishable in the top-hat evolution, because, as we argued before, a spherical mass has almost the same dynamic trajectory in all flat universes with $\Lambda \leq 0.8$. Therefore, with the proper parameters, both SCDM and LCDM are consistent with the abundance and two-point correlation function of C IV systems.

The two CHDMs are in trouble. According to the abundance fitting, the hosting halos of C IV systems should have masses as small as $10^{11} M_{\odot}$. However, the correlation function of such halos is much less than is observed. In order to match the observed correlation function, the halo masses must be at least $10^{12} M_{\odot}$ (Figs. 5c and 5d). But the number of these halos is too few to account for the number of observed C IV systems. Therefore, there are no consistent parameters for CHDM1 and CHDM2 under which both the abundance and correlation tests can passed.

As pointed out by Heisler, Hogan & White (1989), the observed 1-D correlation function may not properly show the real-space correlation but may be amplified somehow by the peculiar velocity. According to their estimation based on a simple model, the amplitude of the correlation function on scales less than the peculiar velocity could be amplified by the factor of $(r_0/r_{cl})^{\gamma}$, where r_0 is the correlation length, γ the correlation index and r_{cl} the cloud radius. Namely, the correlation length is amplified by the factor (r_0/r_{cl}). In the CHDM models, the correlation length of $10^{11} M_{\odot}$ halos is less than 0.1 Mpc at redshift

2.8, so the amplification factor does not exceed 3. Therefore, this mechanism is far from resolving the discrepancy which are found on scales of 3 - 5 h^{-1} Mpc in the CHDMs.

4. Discussion and conclusions

Using the approximate expressions of correlation function and halo's number density in the PS formalism, we have derived constraints on the masses of collapsed halos in four models of structure formation. Generally speaking, because the number density of collapsed halos is inversely dependent on the threshold mass above which the halos are selected, the abundance of C IV systems sets up an upper limit to the threshold mass for their hosts. On the other hand, the 2-point correlation function of collapsed halos is positively dependent on the threshold mass, so the C IV clustering observation sets up a lower limit to the threshold mass. Therefore, a model should be considered inconsistent if the lower limit is found to be larger than the upper limit. The two CHDM models are just such examples. Even when the size of the C IV absorbers is taken to be 5 times larger than that observed, the upper limit ($10^{11} M_{\odot}$) provided by the abundance is still inconsistent with the lower limit ($10^{12} M_{\odot}$) inferred from the correlation.

We note from Fig. 3 that the mass correlation functions of CHDMs are much less than those of SCDM and LCDM. Yet, their corresponding halo correlations are greatly enhanced if we look at the same mass thresholds in Fig. 5. This is due to the large gravitational bias of massive halos in the CHDM models. Could it be possible that other biasing effects can further enhance the correlations, so the models can finally pass the correlation test? The answer probably is negative, because, expect gravitation, there are almost no available bias mechanisms for generating a higher correlation for less mass halos. Hydrodynamical processes generally are ineffective to produce any inhomogeneity on scales equal to or larger than 5 h^{-1}Mpc, as the streaming velocity of gaseous component is only about a thousand km s^{-1} on average.

Changing the density parameter of the hot dark matter from $\Omega_h = 0.3$ (CHDM1) to

0.2 (CHDM2) does not relieve this difficulty much either. Though CHDM2 has a variance 1.2 times that of CHDM1 in the linear evolution, it still cannot produce enough halos hosting C IV systems.

Finally, as pointed out in §2.4, our approximation of the correlation function may give higher power on small scales than some N-body simulations; however, this does not affect the conclusion about the CHDMs models. If Eq. (23) really overestimates the correlation function on small scales, the difference between the models and the observation would be even more significant than is shown in Figs. 5c and 5d. In that case, the difficulty for the models would become more severe.

Acknowledgments Many thanks are due to Houjun Mo for stimulating discussions on the description and application of the Press-Schechter formalism. We are grateful to Van Dixon for his help in improving the quality of the manuscript. HGB is supported by a fellowship of the World Laboratory.

References

* World Lab Fellowship, Beijing Astronomical Observatory, Beijing, P.R. China

??ardeen, J.M., Bond, J.R., Kaiser, N. & Szaley, A.S. 1986, ApJ, 304, 15

??echtold, J., Crotts, P.S., Duncan, R.C. & Fang Y. 1994, ApJ, 437, L83

??ergeron, J. et al. 1994, ApJ, 436, 33

??i, H.G., Ge, J. & Fang, L.Z. 1995, ApJ, 452, 90

??ond, J.R., Cole, S., Efstathiou, G. & Katser, N. 1991, ApJ, 379, 440

??rotts, A.P.S., Bechtold, J., Fang, Y. & Duncan, R.C. 1994, ApJ, 437, L79

??inshaw, N., Impey, C.D., Foltz, C.B., Weymann, R.J. & Chaffee, F.M., 1994, ApJ, 437, L87

??fstathiou, G., Frenk, C.S., White, S.D.M. & Davis, M. 1988, MNRAS, 235, 715

??eisler, J., Hogan, C.J. & White, S.D.M. 1989, ApJ 347, 52

??amilton, A.J.S., Kumar, P., Lu, E. & Matthews, A. 1991, ApJ, 374, L1

??ing, Y.P. & Fang, L.Z. 1994, ApJ, 432, 438

??aiser, N. 1984, ApJ, 284, L9

??lypin, A., Holtzman, J., Primack,J. R. & Regos, E. 1993, ApJ, 416, 1

??lypin, A., Borgani, S., Holtzman, J. & Primack, J. 1995, ApJ, 444, 1

??acey, C., & Cole, S., 1994, MNRAS, 271, 676

??ouis W.C., 1994, in Proceedings of the XVI Conference on Neutrino physics and Astrophysics, Eilat, Israel.

??a, C.P. & Bertschinger, E. 1994, ApJ, 434, L5

??o, H.J. & Miralda-Escudé, J. 1994, ApJ, 430, L25

??o, H.J. & White, S. 1995, preprint

??eebles, P.J.E. 1984, ApJ, 284, 439

??ress, W.H. & Schechter, P. 1974, ApJ, 187, 425

??argent, W.L., Boksenberg, A. & Steidel, C.C. 1988, ApJS, 68, 539

??teidel, C.C. 1990, ApJS, 72, 1

??olfe, A. 1993, in *Relativistic Astrophysics and Particle Cosmology*, eds. Akerlof, C.W. & Srednicki, M.A., N.Y. Academy of Sciences

Table 1. Parameters of the cosmological models

	SCDM	LCDM	CHDM1	CHDM2
h	0.5	0.75	0.5	0.5
Ω_{cb}	1	0.3	0.7	0.8
Ω_h	0	0	0.3	0.2
Λ_0	0	0.7	0	0
$Q_{rms}(\mu K)$	18.0	18.0	18.0	18.0

Figure Captions

Figure 1 Threshold δ_c as a function of the collapsing redshift z_c for $\Omega = 0.9$, 0.7, 0.5, 0.3, 0.1, plotted from top to bottom.

Figure 2 The function $f(x)$ defined by $\delta_0 = \delta_c(1+z)f(r(1+z)/r_0)$ according to Eqs. (14) and (15).

Figure 3 The integrated mass correlation functions in the SCDM, LCDM, CHDM1 and CHDM2 models. The solid lines are calculated from Eqs.(19) and (20). The dotted lines are the linear correlation functions, and the dashed line in the SCDM model is from the empirical formula of Hamilton et al. (1991).

Figure 4a The comoving abundance of collapsed halos with masses greater than M in the SCDM model. The eight curves correspond to $M = 10^{10+0.5n} M_\odot$, $n = 0, 1, ..., 7$, from top to bottom. The bold error bars in the middle are the number densities of QSO C IV absorption systems deduced from 1-D observational data and the measured radius 39 h^{-1} kpc. The data sets above and below the middle ones are the number densities when the radius is (39/5) h^{-1} kpc and (5 × 39) h^{-1} kpc, respectively.

Figure 4b The same as Fig. 4a for the LCDM model.

Figure 4c The same as Fig. 4a for the CHDM1 model.

Figure 4d The same as Fig. 4a for the CHDM2 model.

Figure 5a The correlation function of collapsed halos with masses greater than M in the SCDM model. The eight curves correspond to $M = 10^{10+0.5n}$ $M_\odot$, $n = 0, 1, ..., 7$, from left to right. The histogram with error bars is the measured correlation function of C IV systems.

Figure 5b The same as Fig. 5a for the LCDM model.

Figure 5c The same as Fig. 5a for the CHDM1 model.

Figure 5d The same as Fig. 5a for the CHDM2 model.

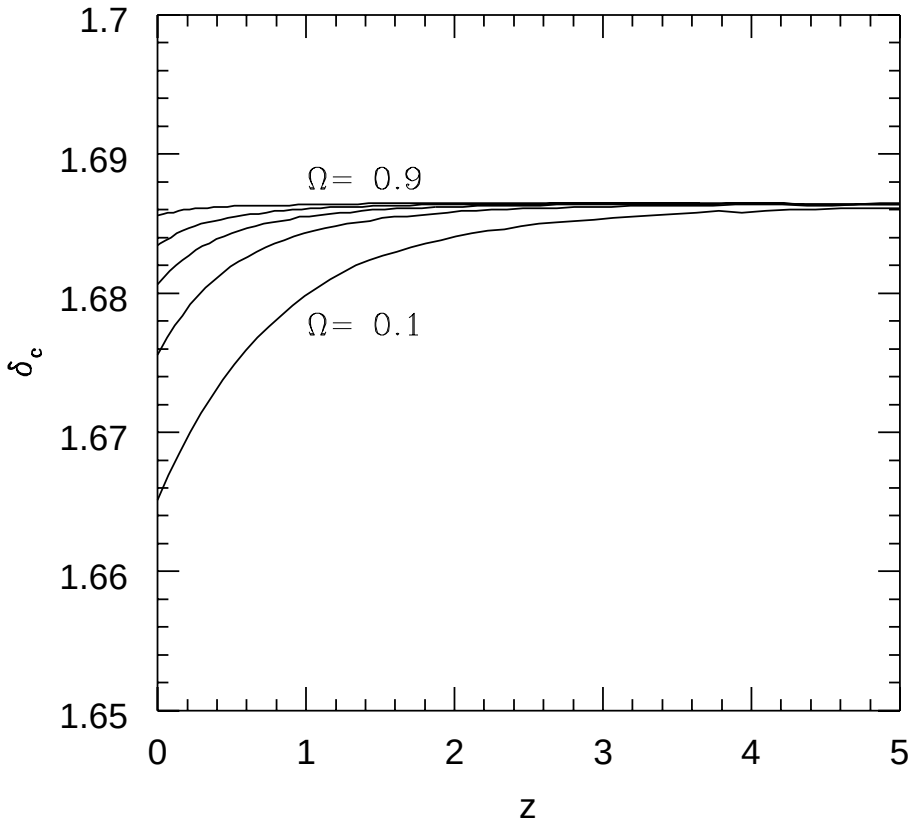

Fig. 1

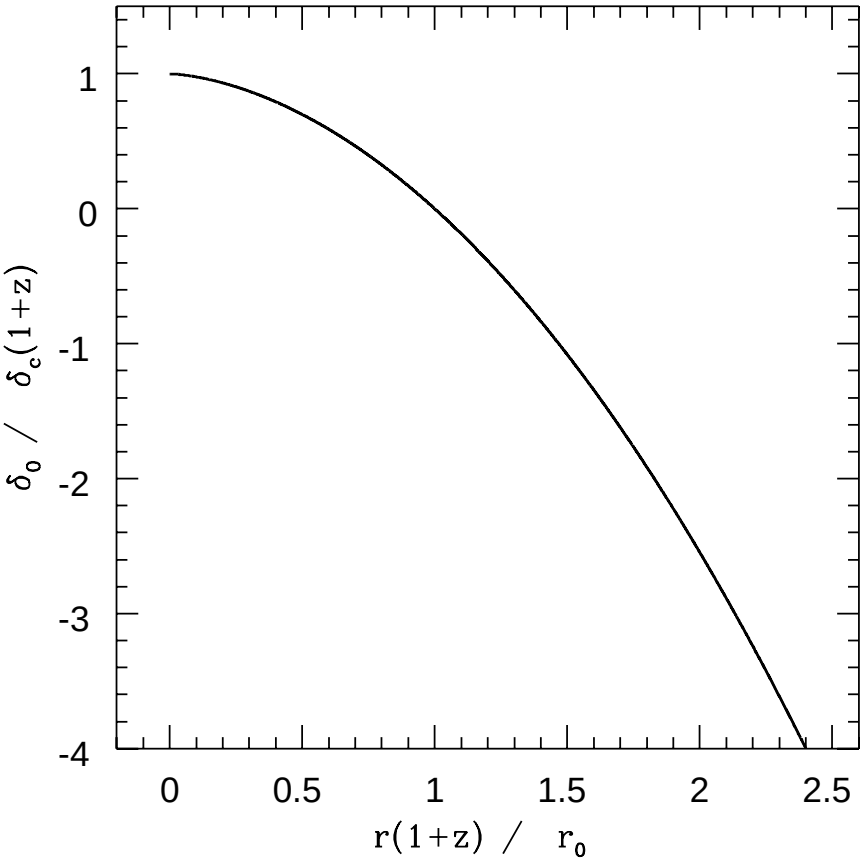

Fig. 2

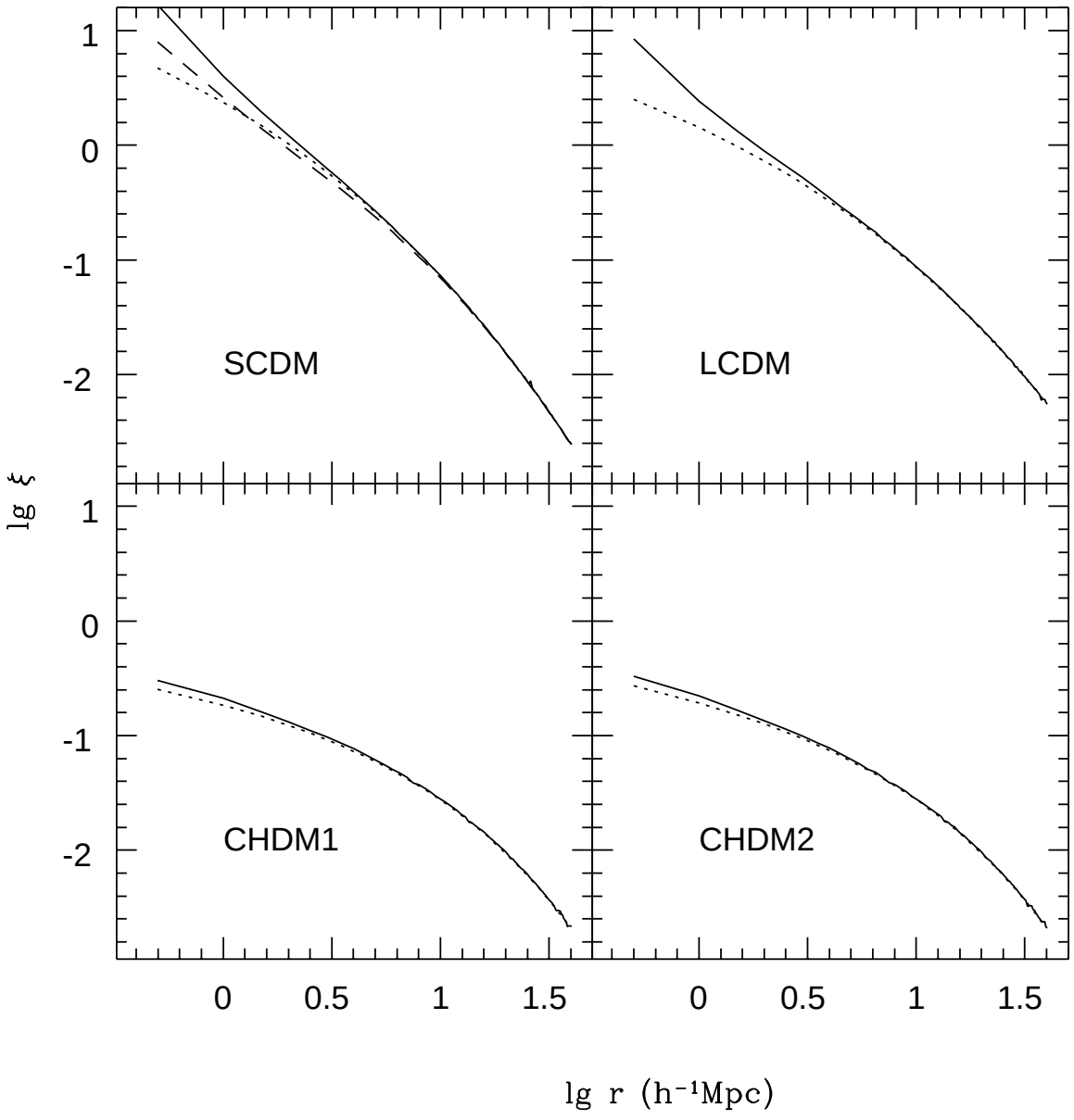

Fig. 3

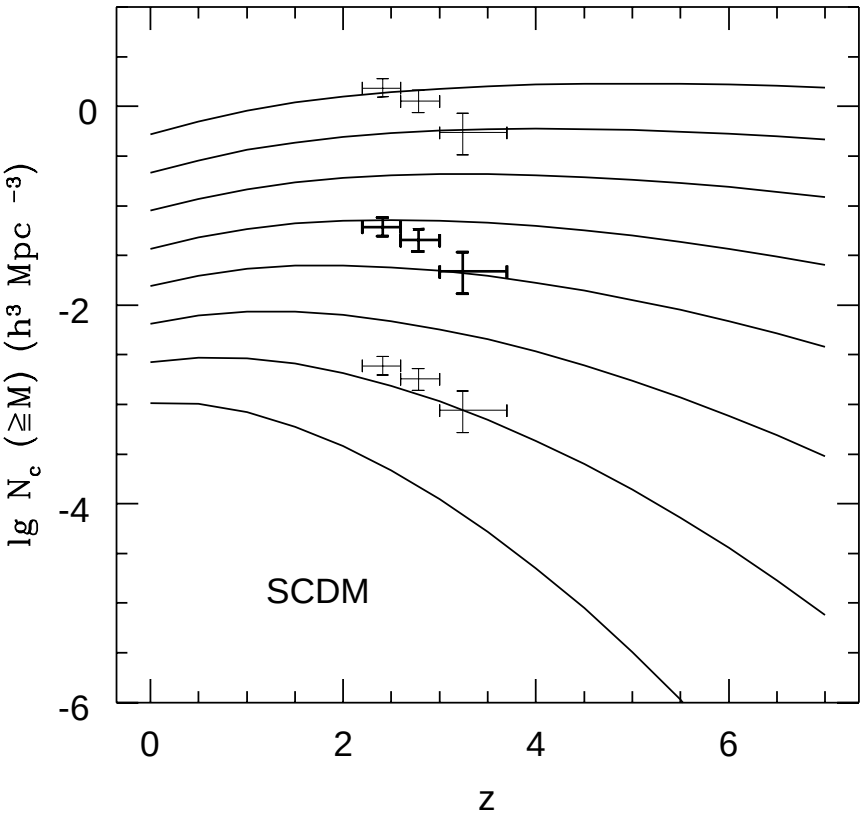

Fig. 4a

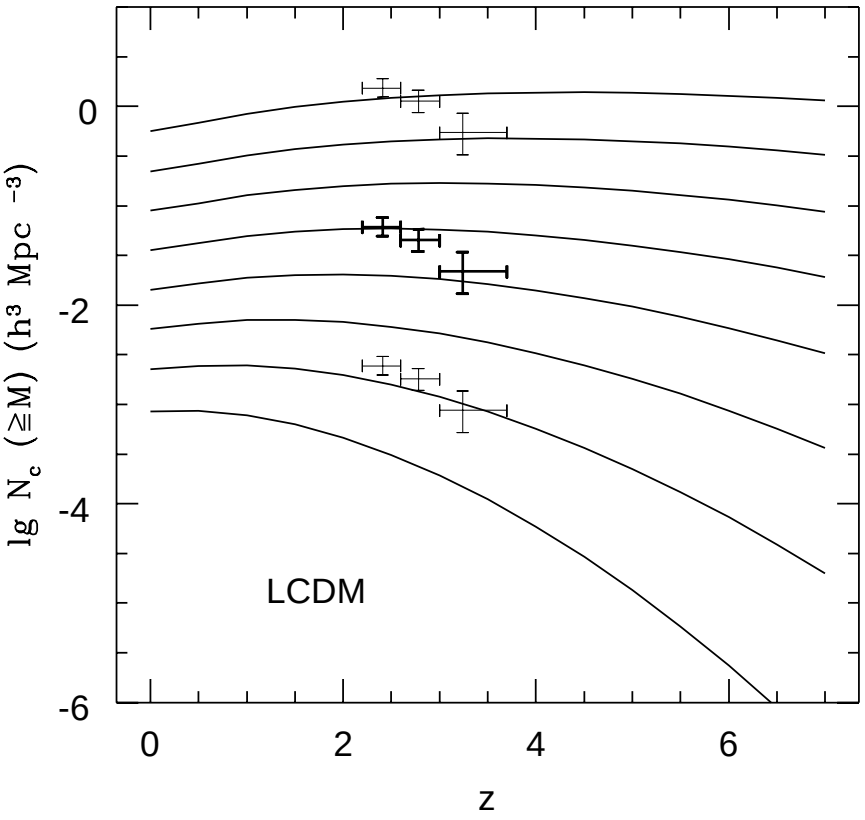

Fig. 4b

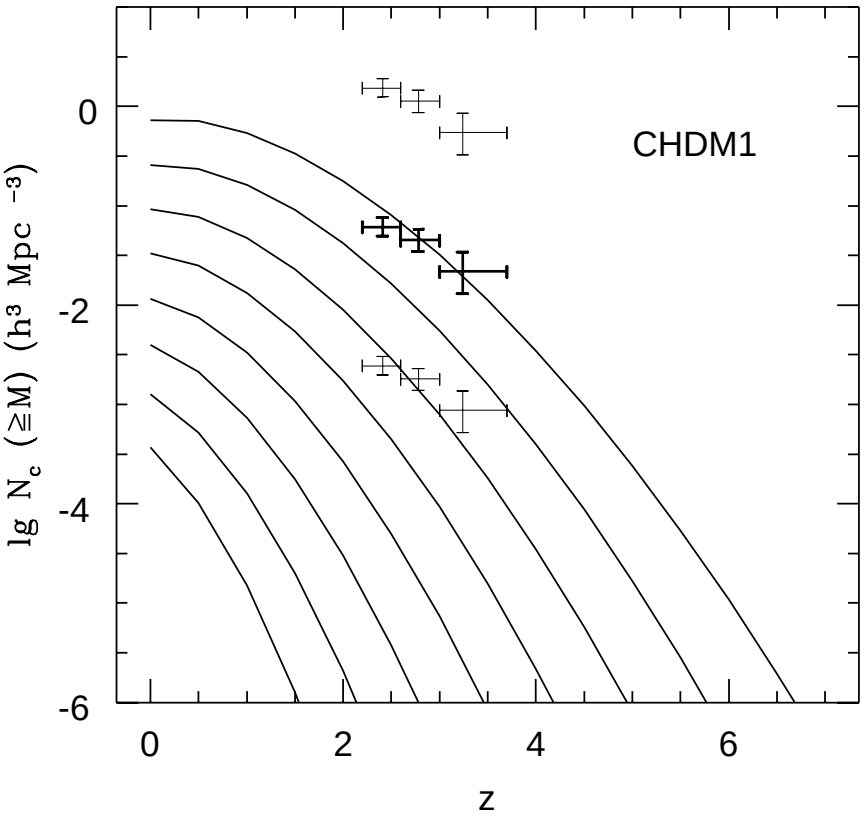

Fig. 4c

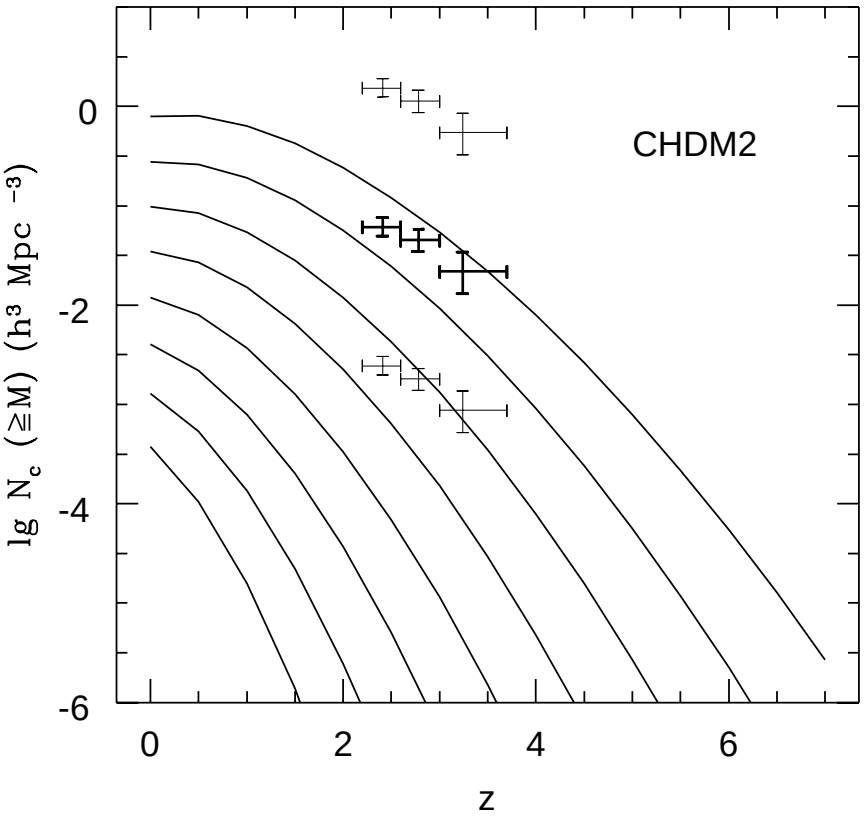

Fig. 4d

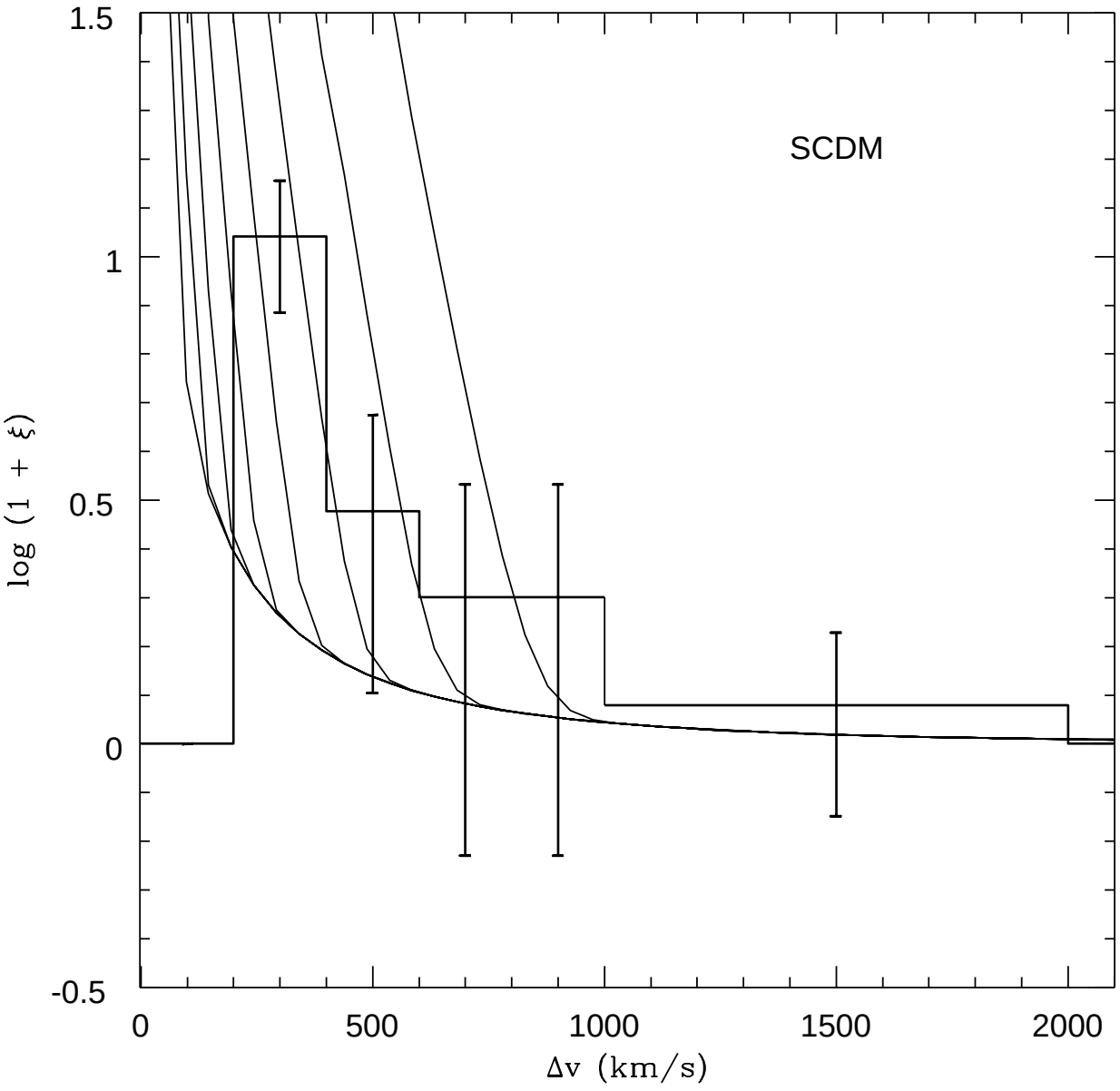

Fig. 5a

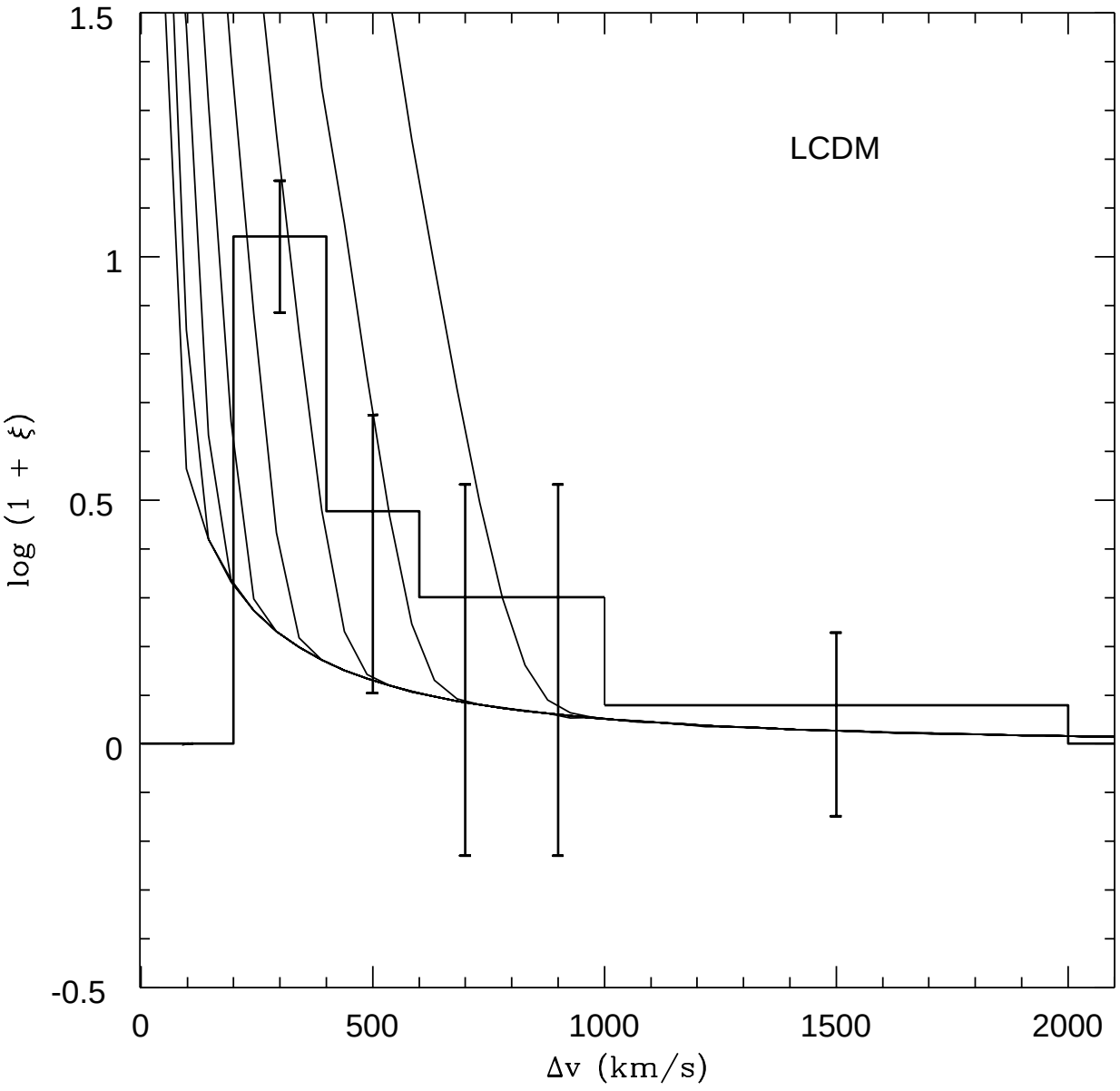

Fig. 5b

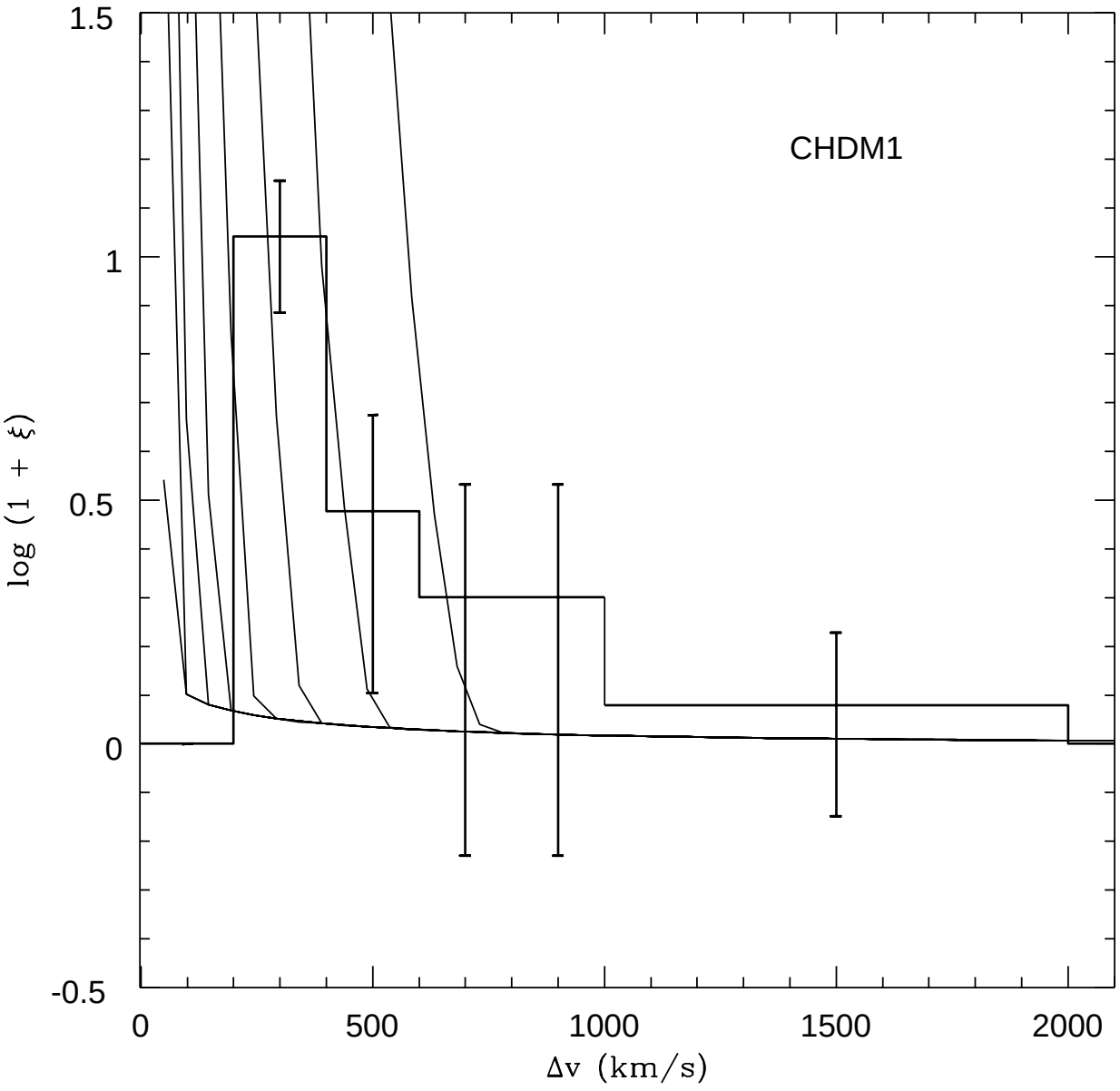

Fig. 5c

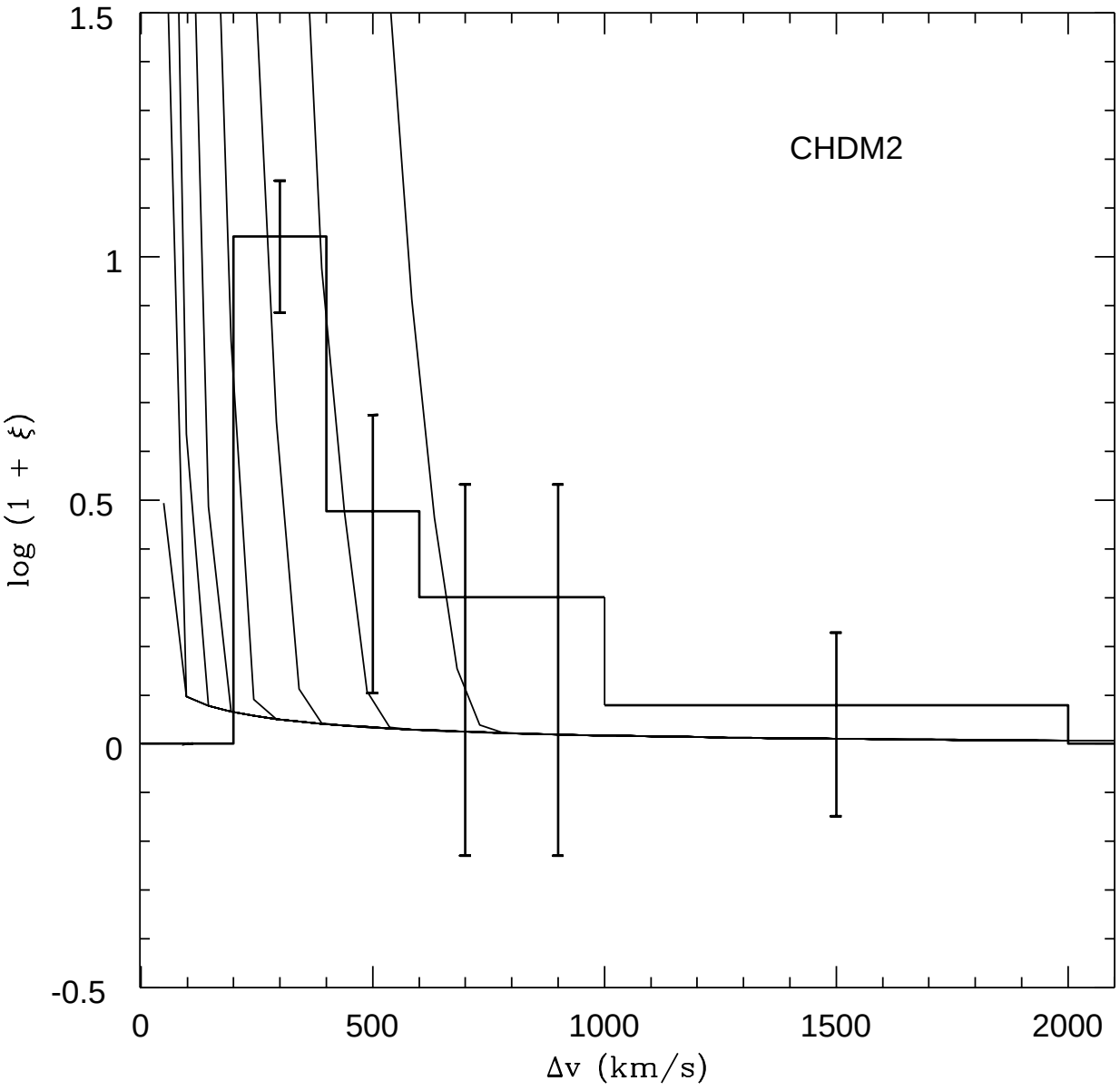

Fig. 5d